

# FRAGILITY AND VULNERABILITY ANALYSIS OF RC BUILDINGS WITH DIFFERENT SHAPES IN THE BASE

Radomir Folić<sup>(1)</sup>, Miloš Čokić<sup>(2)</sup>, Boris Folić<sup>(3)</sup>

<sup>(1)</sup> Professor emeritus, University of Novi Sad, FTS Civil engineering and Geodesy, Novi Sad, Serbia, [folic@uns.ac.rs](mailto:folic@uns.ac.rs)

<sup>(2)</sup> Structural Engineer, Belgrade, Serbia, [cokicmilos@gmail.com](mailto:cokicmilos@gmail.com)

<sup>(3)</sup> Scientific researcher, University of Belgrade, Innovation center, Faculty of Mechanical Engineering, Kraljice Marije 16, Belgrade, Serbia, [boris.r.folic@gmail.com](mailto:boris.r.folic@gmail.com)

## Abstract

In this paper, the seismic response of a three 5 story reinforced concrete (RC) frame system buildings is analysed through the fragility and vulnerability analyses. The constructions are designed in accordance with the structural Eurocodes. All three buildings have the same area, but different shape in the base. For the analysis of the response of structural system to the earthquake actions, the method of nonlinear static (NSA) analysis was applied and based on the obtained results, fragility probability density functions and vulnerability curves were constructed using statistical methods. Structural damage state threshold parameters are determined based on the methodologies described in RISK-UE project. Comparative analysis of the structural damage probability for the three analysed RC buildings is applied in both main directions and as the whole as well. Based on the analysis results, final remarks and conclusions were formulated.

*Keywords:* RC building, seismic nonlinear pushover analyses, fragility, vulnerability, RISK-UE

## 1. Introduction

The behavior of any building depends on the arrangement of structural elements present in it. The important aspects on which the structural configuration depends are geometry, shape and size of the building. Under seismic actions, inertial forces concentrated at the center of mass of the structure, and the vertical bearing element (columns and shear walls) resist the horizontal inertia forces which concentrated at a point called center of stiffness [1].

During an earthquake, failure of structure starts at points of weakness. This weakness arises due to discontinuity in mass, stiffness and geometry of structure. The structures having these discontinuities are termed as irregular structures. Many results of seismic behaviour reinforced concrete (RC) buildings indicate that regularity of their structures considerably affects the structural response with respect to the regular configuration. Regular buildings perform better in earthquakes than do irregular buildings. Irregularities bring down the structural response under seismic loads. However incorporation of some irregularity in structures, during structural design, is inevitable.

Location and size of structural elements have significant effect on torsional coupling which results in damage of structures. Regular structures have no significant discontinuities in plan or in vertical configurations. Structures shall be designed with a clearly defined load path, or paths, to transfer the inertial forces generated in an earthquake to the supporting ground. The building shall be designed to meet the requirements of this subsection and of the design standards referenced in Section 4.2. [2].

Basic principles shall be taken into account in the early stages of the conceptual design of a building and provide structural simplicity, uniformity, symmetry, torsional resistance and stiffness et other. Structural simplicity, characterised by the existence of clear and direct paths for the transmission of the seismic forces. [2]

Uniformity in plan is characterised by an even distribution of the structural elements which allows short and direct transmission of the inertia forces created in the distributed masses of the building. A close relationship between the distribution of masses and the distribution of resistance and stiffness eliminates large eccentricities between mass and stiffness. [2]

A comparative analysis of the behavior of regular and irregular building structures is presented in [3]. Seismic analysis of plan irregular RC building frames is subject of paper [4]. In analysis multimode pushover procedure for the approximate estimation of the seismic response of asymmetric in plan buildings under biaxial seismic excitation described in [5].

This is why analysis of fragility and vulnerability analysis of an RC building is important which is subject paper [6]. In doing so, extensive literature was cited and an overview of the situation was presented. The analysis of numerical analyzes in this paper refers to regular structures of buildings so this paper analyses the constructions of buildings with irregular structures of buildings.

In this paper, the seismic response of a three 5 story RC frame system buildings is analysed through the fragility and vulnerability analyses. The constructions are designed in accordance with the structural Eurocodes: EN1990 [7]; EN1991 [8]; EN1992 [9]; EN1998 [2,10,11], as a ductility class high (DCH) system. All three buildings have the same area, but different shape in the base. For the analysis of the response of structural system to the earthquake actions, the method of nonlinear static (NSA) analysis was applied and based on the obtained results; fragility and vulnerability curves were constructed using statistical methods. Structural damage state threshold parameters are determined based on the methodologies described in RISK-UE project [12]. Comparative analysis of the structural damage probability for the three analysed RC buildings is applied in both main directions and as the whole as well. Based on the analysis results, final remarks and conclusions were formulated.

## 2. Methodology of the analysis and structural modelling

### 2.1 Geometric and material properties of the structure

The subject of the analysis are three office-residential building (Fig. 1, 2 and 3) with 5 levels (ground floor+4 stories). The structural systems exhibits the properties of a frame structural system [2]. The plan view and the 3D model of the structures are shown in Fig. 1, 2 and 3.

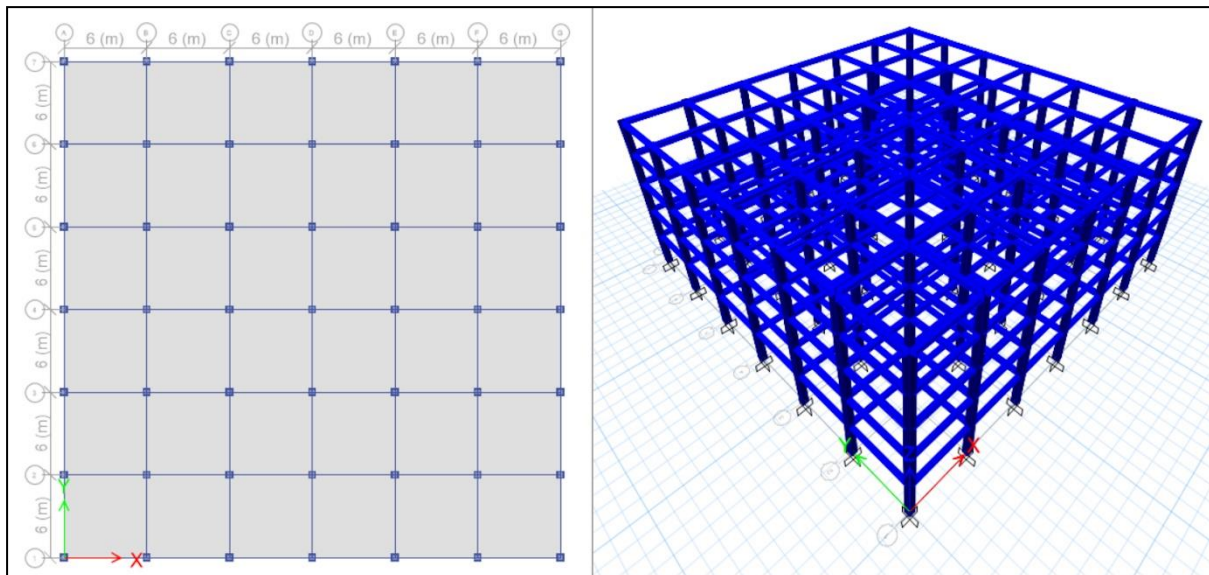


Figure 1. M1: a) Building plan; b) Numerical model [13]

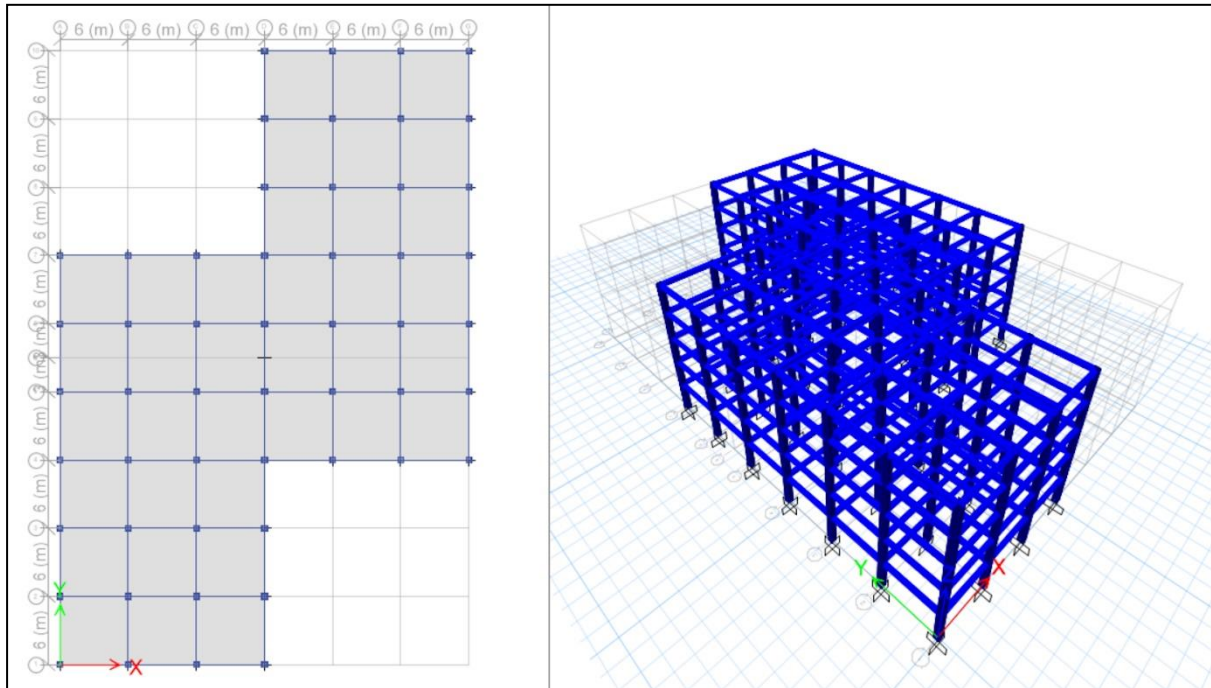


Figure 2. M2: a) Building plan; b) Numerical model [13]

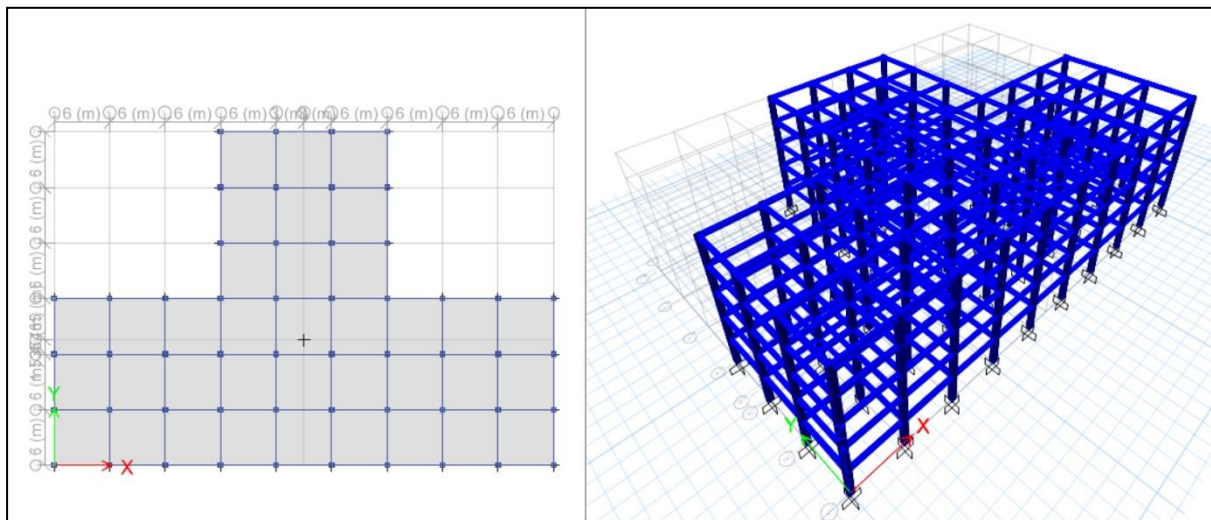


Figure 3. M3: a) Building plan; b) Numerical model [13]

The length of one span in both directions is 6.0 m. The height of the first story is 3.6 m and the height of the other stories is 3.2 m which makes the total height of the building 16.4 m. In order to simplify the modelling and calculation process, all vertical elements are fixed at the bottom level of the structure, i.e. soil-structure interaction is not included in the calculation and design. Characteristics of the structural elements are given in the Table 1.

Table 1 – Geometric characteristics of structural elements

Model	Column $b_c / d_c$ [cm]	Beam $b_b / d_b$ [cm]	Plate $d_{pl}$ [cm]
M1	50 / 50	30 / 40	16
M2	50 / 50	30 / 40	16
M3	50 / 50	30 / 40	16
Long. reinf.	Column $\varnothing_{bL}$ [bar nr. - mm]	Beam $\varnothing_{bL}$ [bar nr. - mm]	Plate $\varnothing_{bL}$ [mm / cm]
M1	16 $\varnothing 14$	3 $\varnothing 22$ 3 $\varnothing 20$	$\varnothing 12/15$
M2	16 $\varnothing 14$	3 $\varnothing 25$ 3 $\varnothing 22$	$\varnothing 12/15$
M3	16 $\varnothing 14$	3 $\varnothing 25$ 3 $\varnothing 22$	$\varnothing 12/15$
Stirrups	Column $\varnothing_{sw}$ [bar nr. - mm / cm]	Beam $\varnothing_{sw}$	Plate /
M1	3 $\varnothing 10/10$	2 $\varnothing 10/10$	/
M2	3 $\varnothing 10/10$	2 $\varnothing 10/10$	/
M3	3 $\varnothing 10/10$	2 $\varnothing 10/10$	/

### 3. Methodology of the analysis and structural modelling

#### 3.1 Geometric and material properties of the structure

Tables For calculation and design of the structure in [13], a spatial (3D) model was used. The following parameters, assumptions and simplifications were adopted:

- The calculation includes the effects of second order logic ( $P-\Delta$ );
- Occurrence of cracks in structural elements was included in the calculation with the stiffness reduction of the elements according to [2].
- The elastic bending stiffness and shear stiffness of columns and beams was reduced to 50%;
- Torsion stiffness of columns and beams was reduced to 10% of their elastic stiffness;
- The elastic stiffness of the RC plate was reduced to 50%.

#### 3.2 Model for nonlinear analysis

In models for post-elastic analysis of structural response to the removal of individual vertical elements, the following assumptions and simplifications were used:

- The calculation includes the effects of second order logic ( $P-\Delta$ );
- To describe the nonlinear behaviour of the material, the nonlinear properties of the material were used to describe the behaviour of concrete (Fig. 4, left) and reinforcement steel (Fig. 4, right) [2], [10], [14];
- Columns and beams were modelled as confined RC elements with a protective layer of concrete (Fig. 4, left) [10]. [14];
- RC plates are modelled as rigid diaphragms in seismic analysis.

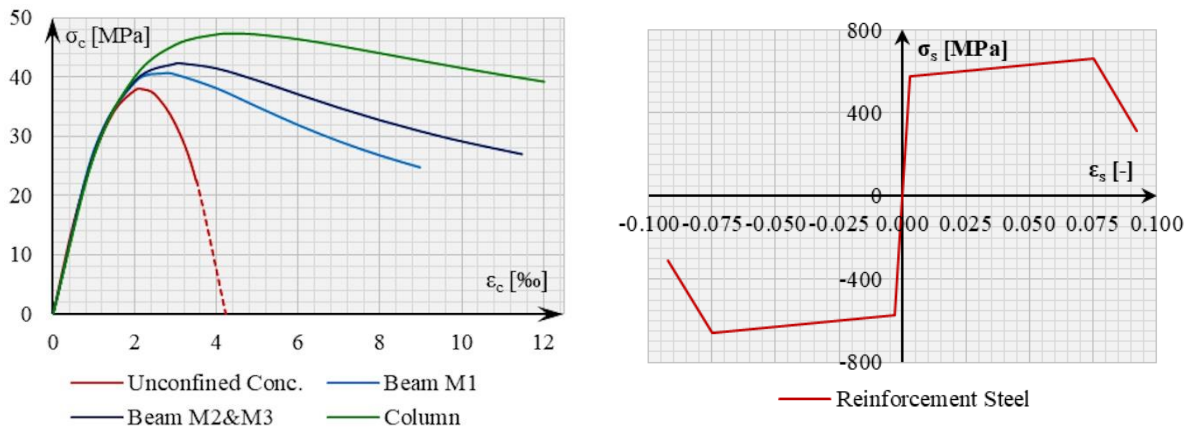


Figure 4. Material properties of concrete (left) and rebar (right)

### 3.3 Properties of plastic hinges

Plastic hinges are modelled as fiber cross sections. They are modelled by automatic selection of fiber division in the cross section of elements [13] for seismic analysis. The lengths of plastic hinges, are equal to the relative lengths of columns and beams of  $0.2L$ , where  $L$  is the length of the element. Therefore, the locations of the hinges are assigned as  $0.1L$  and  $0.9L$  to columns and beams.

## 4. Non-linear analysis results and calculation of fragility curves

### 4.1 Nonlinear static pushover analysis

The results of NSA for modal (MOD) load distribution are shown in Fig. 5. Modal pushover curve was chosen as a referent curve for the calculation of fragility curves, according to [12].

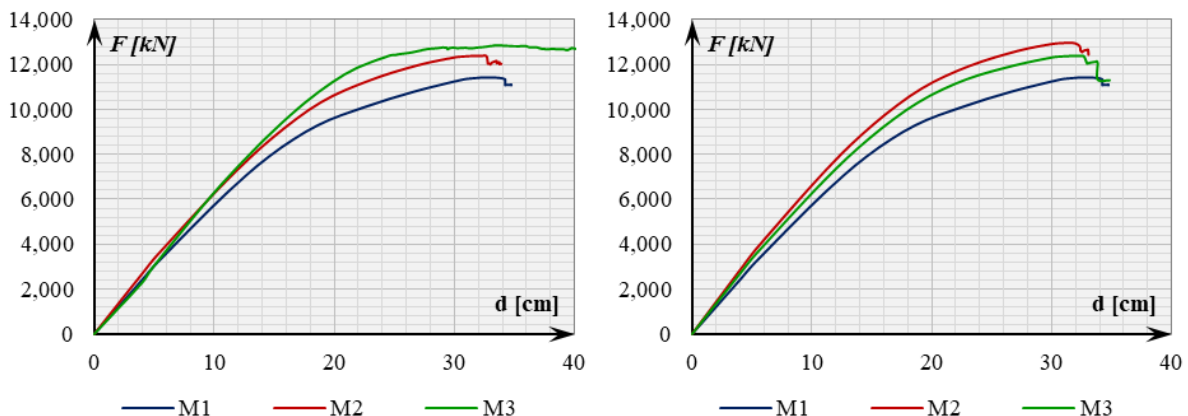


Figure 5. Pushover curves for X (left) and Y direction (right)

The results of pushover analysis for MDOF systems show different responses in both main directions. In the X direction, the structural response of M3 will be somewhat stronger than M2 and in the end M1, while in the Y direction, the response of M2 is better than M3 and then M1.

To calculate damage state (DS) threshold values, it was necessary to do a bilinear approximation of NSA pushover curve, using Equivalent Energy Elastic-Plastic (EEEP) method and determine yielding ( $S_{dY}, S_{aY}$ ) and ultimate capacity ( $S_{dU}, S_{aU}$ ) points on capacity (spectral displacement – spectral acceleration) curve of SDOF system for M1, M2 and M3 (Fig. 6).

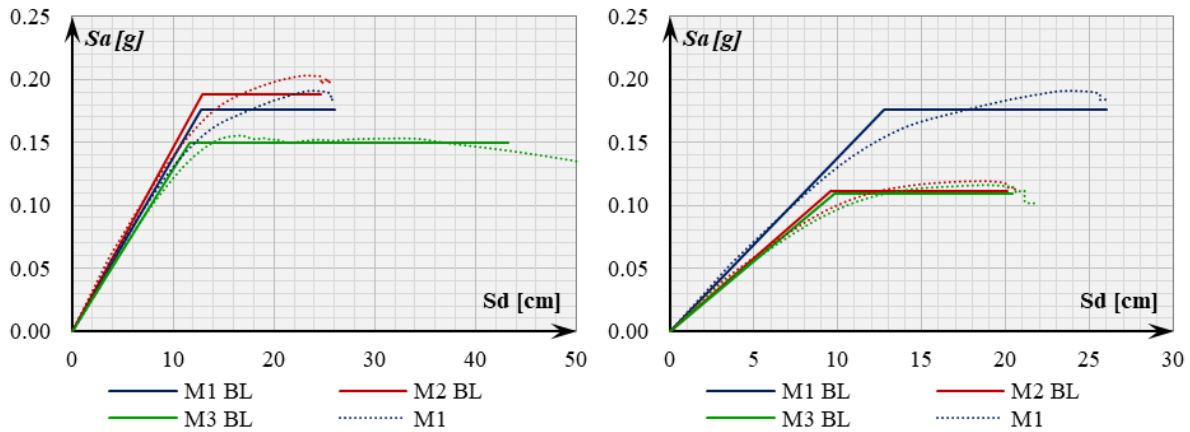


Figure 6. Capacity curves and their bilinear approximation for X (left) and Y direction (right)

The capacity curve comparison results for SDOF systems show different responses in both main directions. In the X direction, the structural response of M2 will be somewhat stronger than M1 and in the end M3, but M3 will give the most ductile response, while in the Y direction, the response of M1 is better and more ductile than M2 and then M3, which are very similar.

The results of NSA are shown in Figure 7. for target displacement ( $d_t$ ) and target spectral displacement ( $Sd_t$ ), for the design PGA = 0.2g. The displacement and spectral displacement values for the three models for the design PGA can be described through the relations:  $d_{t,X}^{M3} > d_{t,X}^{M1} > d_{t,X}^{M2}$  in X and  $d_{t,Y}^{M3} > d_{t,Y}^{M2} > d_{t,Y}^{M1}$  in Y direction for MDOF and  $Sd_{t,X}^{M3} > Sd_{t,X}^{M1} > Sd_{t,X}^{M2}$  in X and  $Sd_{t,Y}^{M3} > Sd_{t,Y}^{M2} > Sd_{t,Y}^{M1}$  in Y direction for MDOF.

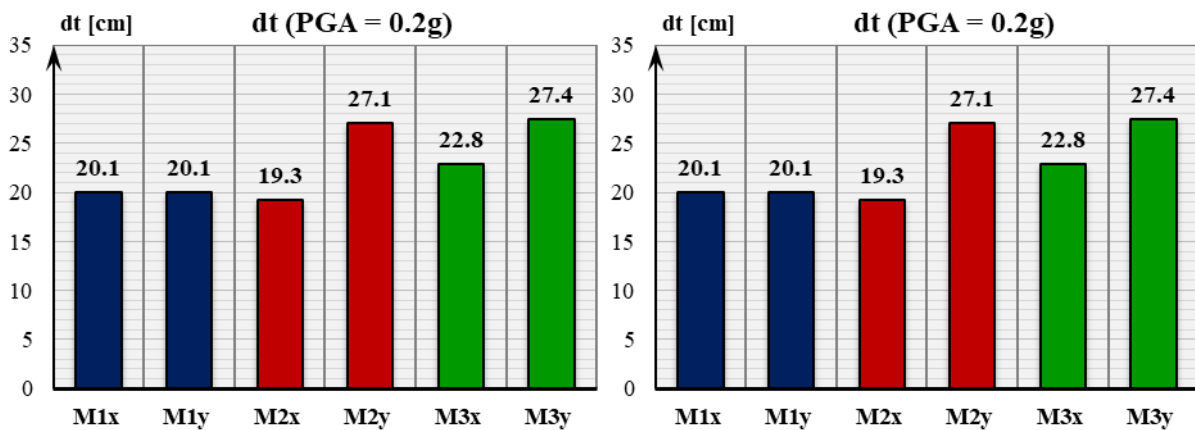


Figure 7. Target displacement and spectral target displacement points

#### 4.2 Damage state performance points

Damage of a structural system may be quantified through threshold performance points (small damage – SD; moderate damage – MD; extensive damage – ED; complete damage – CD), which are determined according to [12] for seismic fragility analysis (Table 1).

Table 1 – Seismic structural DS threshold values, according to [12]

<i>DS</i>	<i>SD [M1 / M2 / M3]</i>			<i>MD [M1 / M2 / M3]</i>			<i>RD [M1 / M2 / M3]</i>			<i>CD [M1 / M2 / M3]</i>		
$\mu_{DS}$	$0.7 \cdot Sd_Y$			$Sd_Y$			$Sd_Y + 0.25 \cdot (Sd_U - Sd_Y)$			$Sd_U$		
$\sigma_{LN,DS}$	$0.25 + 0.07 \cdot \ln(\mu_U)$			$0.2 + 0.18 \cdot \ln(\mu_U)$			$0.1 + 0.4 \cdot \ln(\mu_U)$			$0.15 + 0.5 \cdot \ln(\mu_U)$		
<i>X direction</i>												
$\mu_{DS}^{Sd} [cm]$	8.92	9.00	8.10	12.75	12.85	11.58	16.06	15.80	19.48	25.99	24.64	43.20
$\mu_{DS}^{PGA} [g]$	0.122	0.128	0.107	0.172	0.179	0.150	0.213	0.216	0.249	0.331	0.329	0.590
$\sigma_{LN,DS} [g]$	0.300	0.296	0.342	0.328	0.317	0.437	0.385	0.360	0.627	0.506	0.475	0.808
<i>Y direction</i>												
$\mu_{DS}^{Sd} [cm]$	8.92	6.69	6.84	12.75	9.56	9.77	16.06	12.20	12.43	25.99	20.10	20.40
$\mu_{DS}^{PGA} [g]$	0.122	0.085	0.085	0.172	0.118	0.119	0.213	0.148	0.148	0.331	0.239	0.239
$\sigma_{LN,DS} [g]$	0.300	0.302	0.302	0.328	0.334	0.333	0.385	0.395	0.394	0.506	0.521	0.518

### 4.3 Statistical analysis of the results

It is generally assumed that fragility curve is a lognormal distribution function, which means that “If a variable is log-normally distributed, its natural logarithm is normally distributed. Which means it must take on a positive real value, and the probability of it being zero or negative is zero.” [15] For seismic fragility analysis, lognormal distribution is adopted [12].

### 4.4 Calculation of fragility curves

In case of the calculation of fragility curves, using spectral displacement (*Sd*) as a referent IM value for the DS threshold [12], the fragility functions are calculated as analytical cumulative distribution functions (CDF) for lognormal (LN) distribution:

$$P_{DS_i|IM}(IM_j, \mu_{LN|DS_i}^{IM}, \sigma_{LN|DS_i}^{IM}) = \Phi \left[ \frac{1}{\sigma_{LN|DS_i}^{IM}} \cdot \ln \left( \frac{IM}{\mu_{LN|DS_i}^{IM}} \right) \right] = \Phi \left( \frac{\ln IM - \mu_{LN|DS_i}^{IM}}{\sigma_{LN|DS_i}^{IM}} \right) \quad (1)$$

where  $\Phi$  is the cumulative distribution function of the standard normal distribution,  $\mu_{LN|DS_i}^{IM}$  and  $\sigma_{LN|DS_i}^{IM}$  are the mean and standard deviation of LN distribution values shown in Table 2. However, because it is possible to determine the relation between *Sd* and PGA, it is possible to present the fragility curves with the PGA as the IM.

Probability density function values for the exceedance of different states of damage for the design PGA = 0.2g (Fig. 10, 13 and 16) are calculated using the equations [15], [16]:

$$\begin{aligned} P_{DS_0} &= 1 - P_{DS_1}[IM_j, \mu_{LN|DS_1}, \sigma_{LN|DS_1}] \\ P_{DS_i} &= P_{DS_i}[IM_j, \mu_{LN|DS_i}, \sigma_{LN|DS_i}] - P_{DS_{i+1}}[IM_j, \mu_{LN|DS_{i+1}}, \sigma_{LN|DS_{i+1}}] \\ P_{DS_n} &= P_{DS_n}[IM_j, \mu_{LN|DS_n}, \sigma_{LN|DS_n}] \end{aligned} \quad (2)$$

where  $P_{DS_0}$  is a probability of no damage to occur and  $i = 1, \dots, n$  and  $IM_j = (0.1g - 1.0g)$ .  $i$  is an index of a particular DS, and  $j$  is an index of a particular IM (PGA).  $n$  is a total number of damage states. Probability density functions for damage state exceedance in both main X and Y directions are shown in Figures 8 - 12. As a result, the values of probability for the exceedance of each damage state for all three models in both main directions are given in Figures 13 and 14, for the design PGA = 0.2g.

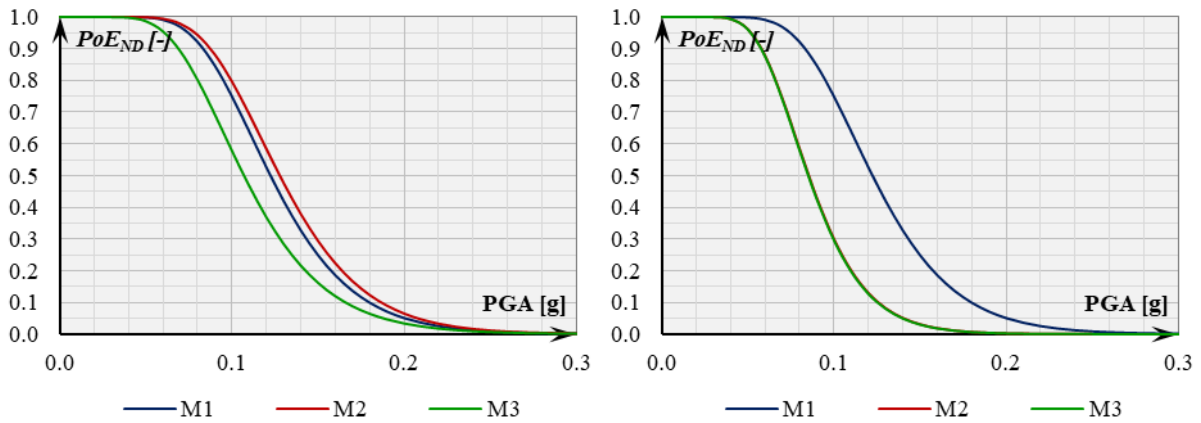


Figure 8. Probability density functions for damage state exceedance probability for ND in X (left) and Y direction (right)

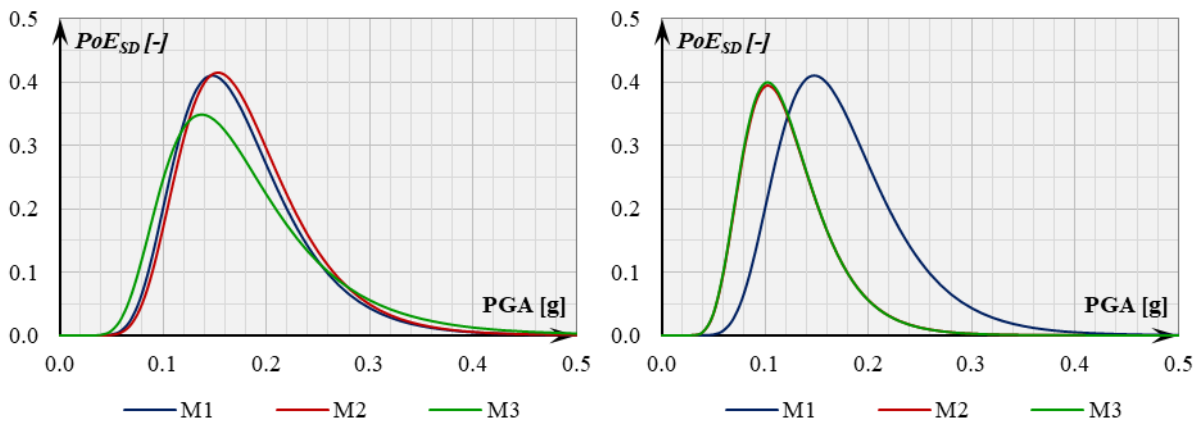


Figure 9. Probability density functions for damage state exceedance probability for SD in X (left) and Y direction (right)

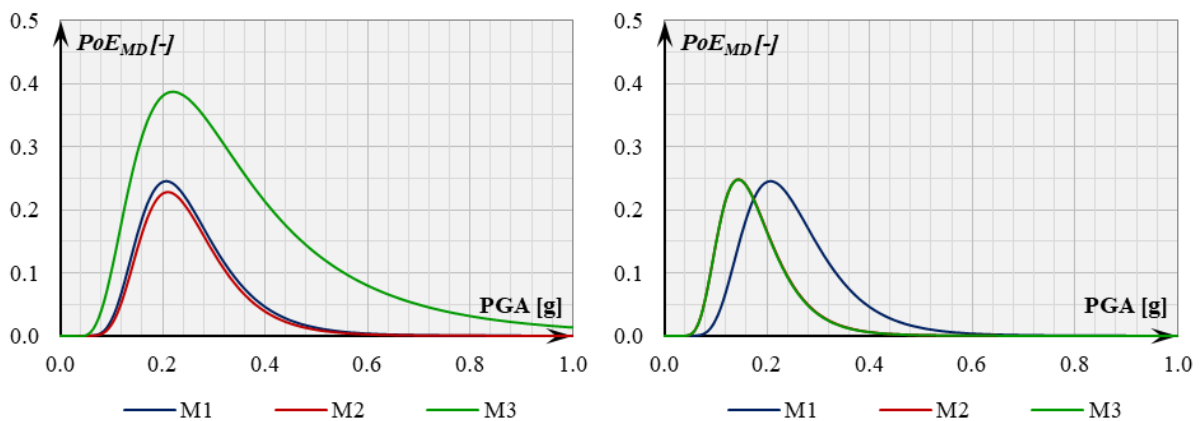


Figure 10. Probability density functions for damage state exceedance probability for MD in X (left) and Y direction (right)



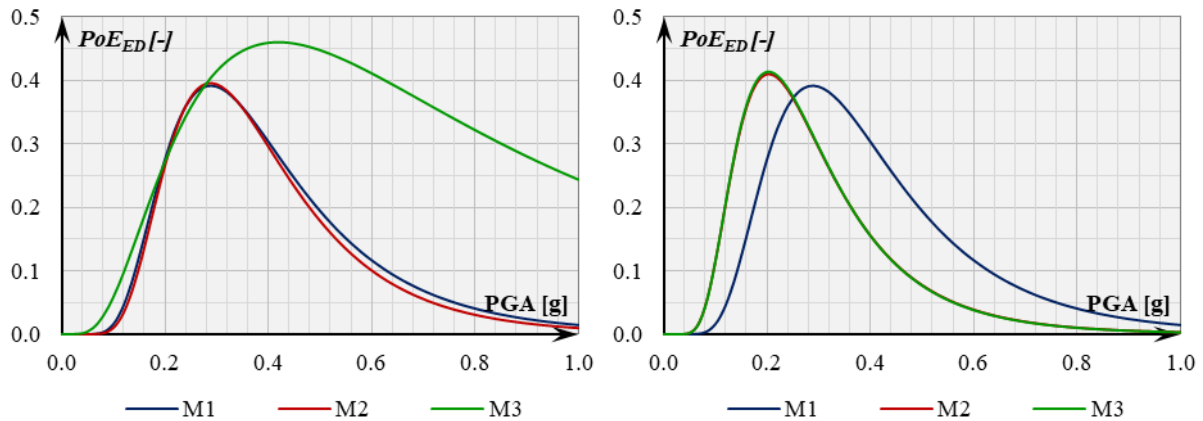


Figure 11. Probability density functions for damage state exceedance probability for ED in X (left) and Y direction (right)

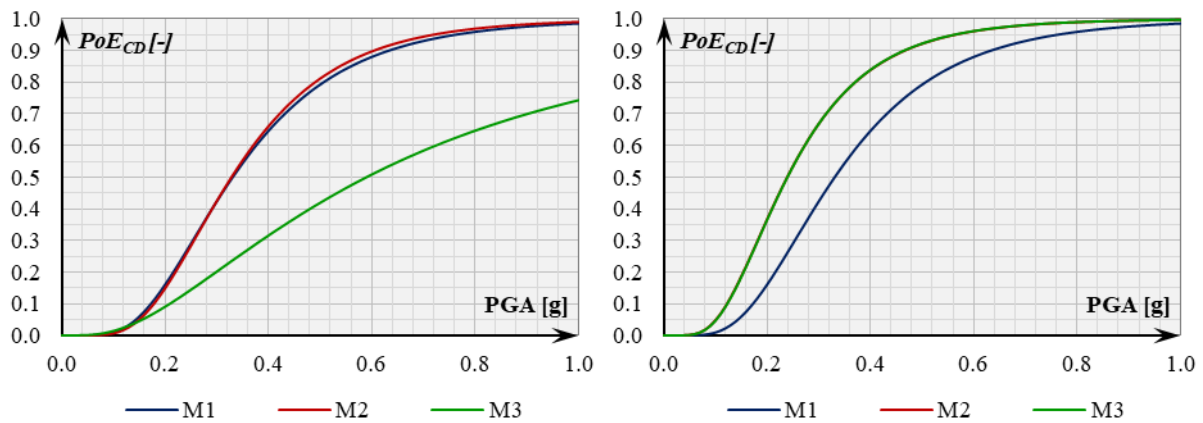


Figure 12. Probability density functions for damage state exceedance probability for CD in X (left) and Y direction (right)

Damage state exceedance probability values in X direction for the design PGA = 0.2g are shown in Figure 13. From the aspect of damage states, it can be noticed that M1 and M2 show the similar response for the seismic action in X direction for the design PGA intensity. However, M1 is a bit more prone than M2 to ED (3.4%) and to CD (8.1%). M3 shows much better response than M1 and M2 for the seismic action in X direction for the design PGA intensity. While it is much more prone to exceed the level of MD than M1 (56.1%) and M2 (68.6%), it has much lower probability to exceed CD than M1 (-43.8%) and M2 (-39.2%).

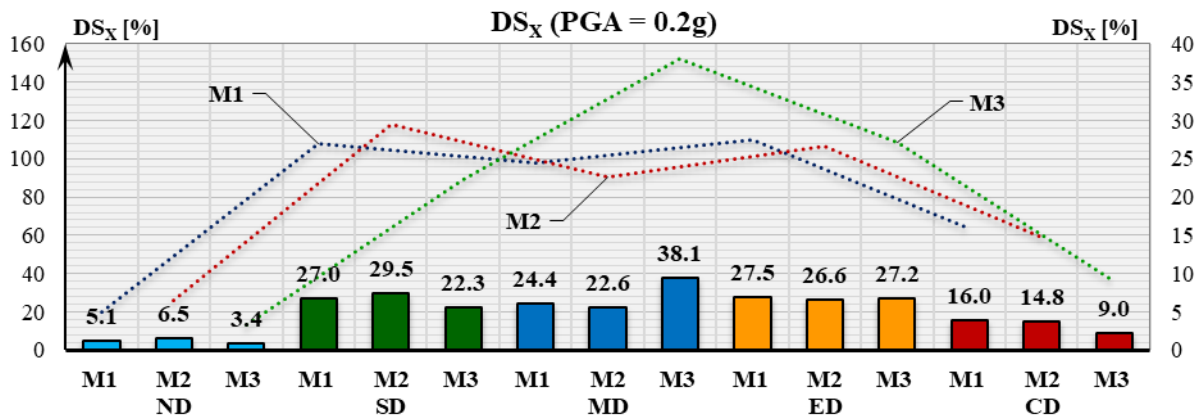


Figure 13. Damage state exceedance probability in X direction for the design PGA

Damage state exceedance probability values in Y direction for the design PGA = 0.2g are shown in Figure 14. From the aspect of damage states, it can be noticed that M2 and M3 show very similar or almost the same response for the seismic action in Y direction for the design PGA intensity. The difference between the response of M2 and M3 varies from 0.1% - 0.3% in probability. M1 shows much better response than M2 and M3 for the seismic action in Y direction for the design PGA intensity. While it is much more prone to exceed the level of SD and MD than M2 (-79.3% and -32.0%) and M3 (-79.6% and -32.8%), it has much lower probability to exceed ED and CD than M2 (-32.9% and -56.3%) and M3 (-33.4% and -56.0%).

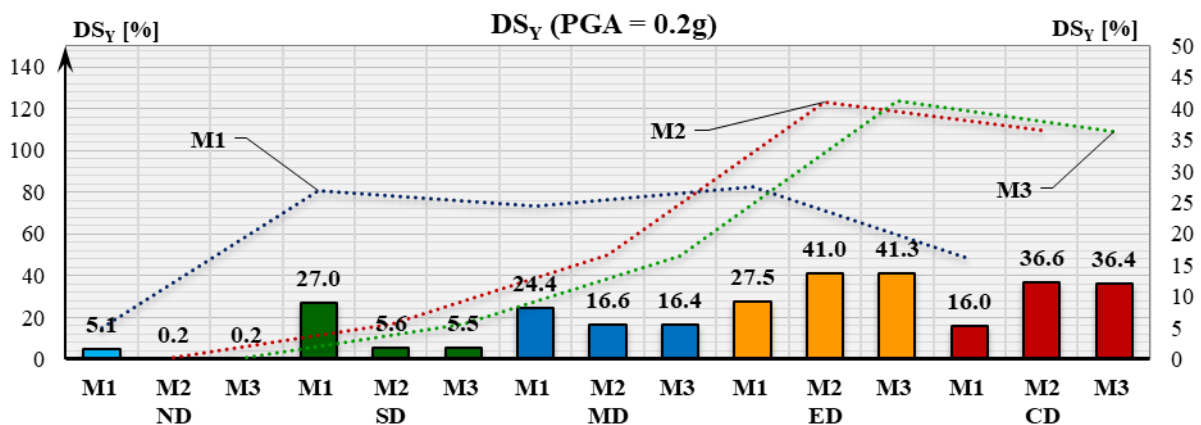


Figure 14. Damage state exceedance probability in Y direction for the design PGA

Damage state exceedance probability values in Y direction for the design PGA = 0.2g are shown in Figure 14. From the aspect of damage states, it can be noticed that M2 and M3 show very similar or almost the same response for the seismic action in Y direction for the design PGA intensity. The difference between the response of M2 and M3 varies from 0.1% - 0.3% in probability. M1 shows much better response than M2 and M3 for the seismic action in Y direction for the design PGA intensity. While it is much more prone to exceed the level of SD and MD than M2 (-79.3% and -32.0%) and M3 (-79.6% and -32.8%), it has much lower probability to exceed ED and CD than M2 (-32.9% and -56.3%) and M3 (-33.4% and -56.0%).

In order to calculate the seismic response of each model for both directions, the values of probability of damage state exceedance and vulnerability mean damage values (MDF) are calculated using geometric mean equation:

$$\left(\prod_{i=1}^n x_i\right)^{\frac{1}{n}} = \sqrt[n]{x_1 \cdot x_2 \cdot \dots \cdot x_n} \quad (3)$$

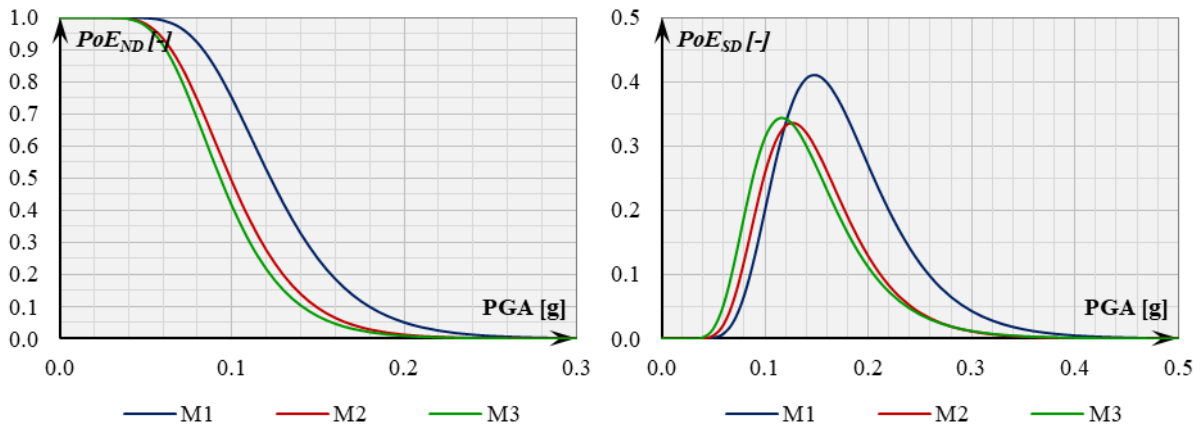


Figure 15. Probability density functions for damage state exceedance probability for ND (left) and SD (right), geometric mean for both directions

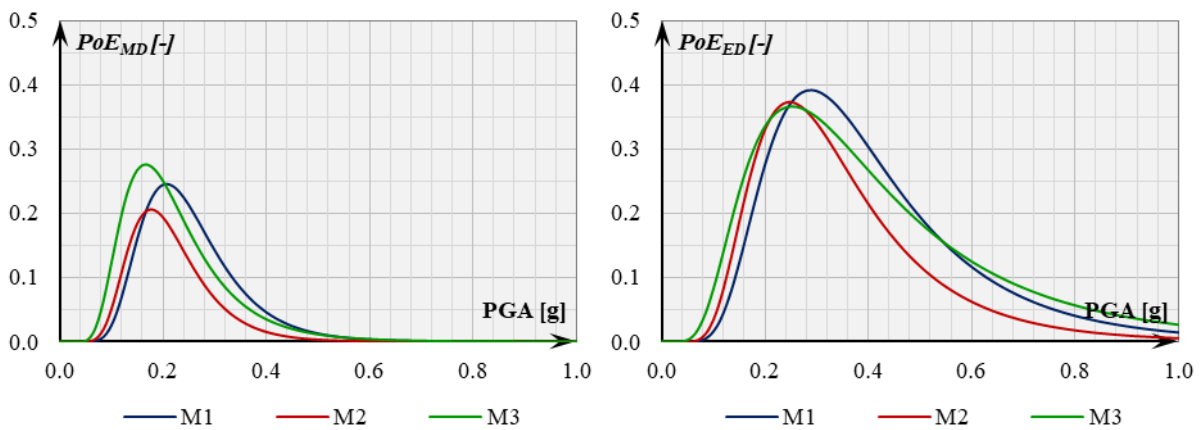


Figure 16. Probability density functions for damage state exceedance probability for MD (left) and ED (right), geometric mean for both directions

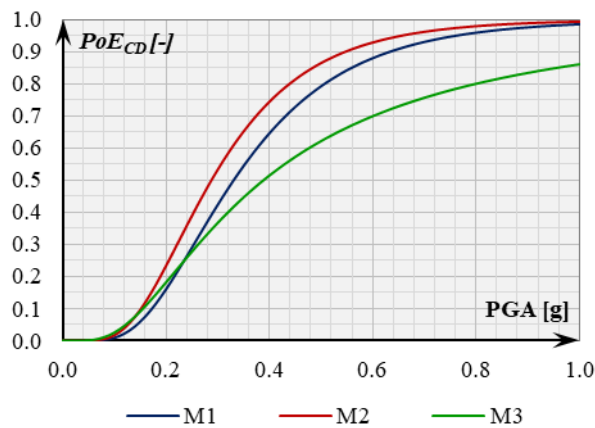


Figure 17. Probability density functions for damage state exceedance probability for CD, geometric mean for both directions

Damage state exceedance probability geometric mean values for both directions for the design PGA = 0.2g are shown in Figure 18. From the aspect of damage states, it can be noticed that in general, M1 has better response than M3, which has a similar, but slight better response than M2. The percentual comparison of values of M2 and M3 to M1 as a referent model is given in Table 3.

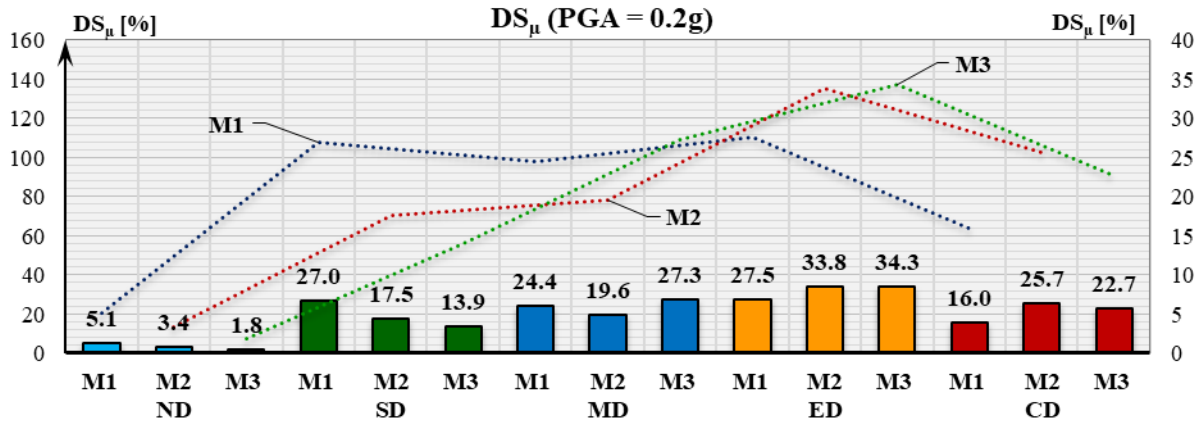


Figure 18. Damage state exceedance probability for the design PGA, geometric mean for both directions

Table 3 – Comparison of PoE values of M2 and M3 to M1

DS [%]	ND <sub>μ</sub>	SD <sub>μ</sub>	MD <sub>μ</sub>	ED <sub>μ</sub>	CD <sub>μ</sub>
M1	0.00	0.00	0.00	0.00	0.00
M2	-33.75	-34.93	-19.83	22.67	60.88
M3	-64.47	-48.39	11.58	24.47	42.24

#### 4.5 Vulnerability analysis

Calculation process of vulnerability curves was performed according to the method described in [17]. Calculation of the vulnerability curves, based on the fragility results was done according to the equation and process described in paper [17]:

$$E(C|IM) = \sum_{i=0}^n E(C|DS_i) \cdot P(DS_i|IM) \quad (3)$$

where  $n$  is the number of considered DS ( $DS_i$ ),  $P(DS_i|IM)$  is the damage probability;  $E(C|DS_i)$  and  $E(C|IM)$  are the cumulative distribution of cost (or loss) according to [17]. The values of  $E(C|DS_i)$  are adopted from [17]. The results are compared and displayed in Figures 19 and 20.

Table 4 – Damage factor functions of building typology according to [17]

Damage Scale	$E(C DS_i)$			
	Slight (SD)	Moderate (MD)	Extensive (ED)	Complete (CD)
Damage State	2%	10%	50%	100%

Vulnerability MDF values in X and Y direction for the design PGA = 0.2g are shown in Figure 20. It can be noticed that M1 and M2 have very similar or almost the same response for the seismic action in X direction (Figure 19, left and Figure 21, left) for the design PGA intensity and that M3 have much better response than both M1 and M2. In Y direction (Figure 19, right and Figure 21, left), M1 has

better response than both M2 and M3, which both have almost the same response for the seismic action. Regarding the comparison of the models in both directions from the aspect of geometric mean values (Figure 20 and Figure 21, right), M1 has the best response, after which is M3 and then M2. However, for the value of  $PGA > 0.3g$  (Figure 20), the response of M3 is better than M1 and M2

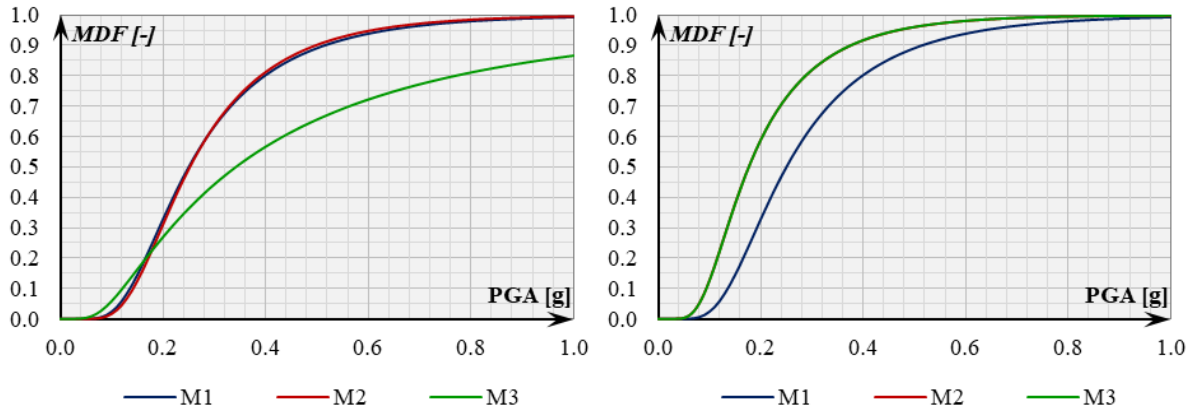


Figure 19. Vulnerability curves for X (left) and Y direction (right)

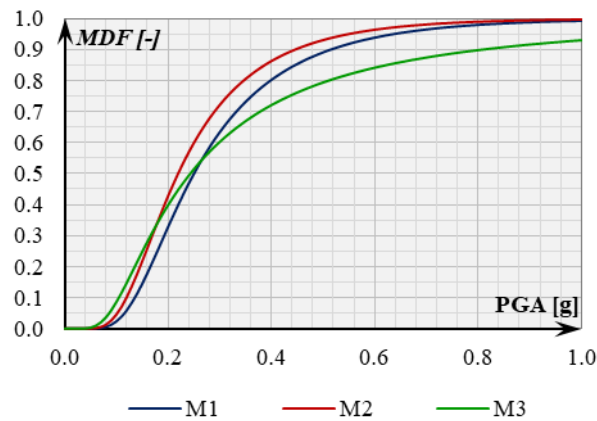


Figure 20. Vulnerability curves geometric mean values for both directions

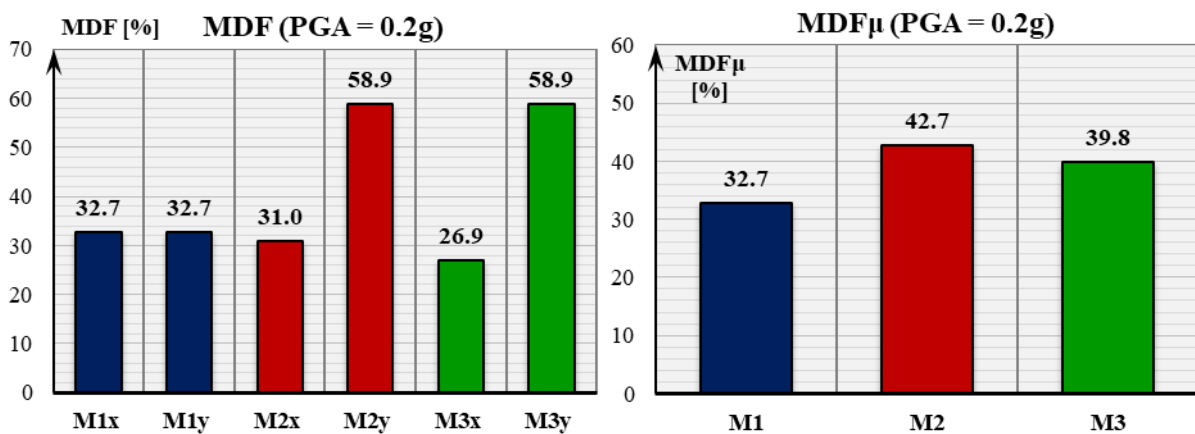


Figure 21. MDF for both directions (left) and MDF values mean for both directions (right) for design PGA

## 5. Conclusions

In this paper, the fragility and vulnerability of a three 5 story RC frame system buildings exposed to seismic action is analysed through their nonlinear response. The constructions are designed in accordance with the structural Eurocodes, as DCH systems. The common characteristic of all three buildings are: the same area and the same number of stories, but different shape in the base. For the analysis of the response of structural system to the earthquake actions, the method of nonlinear static (NSA) analysis was applied and based on the obtained results; fragility functions, probability density functions for damage state exceedance probability and vulnerability curves were calculated using statistical methods. Comparative analysis of the structural damage probability for the three analysed RC buildings is applied in both main directions and as the whole as well, using the geometric mean values. Based on the analysis results, some conclusions may be formulated:

- In the main X direction, M2 shows a bit better characteristics than M1, which can be explained by the arrangement of the elements in the structure and the distribution of mass and inertial forces induced by seismic action. M3 has much better performance in the X direction than both M1 and M2, because it's resisting to seismic action with a longer, stiffer frames in the part of the structure.
- In the main Y direction, M1 shows much better response than both M2 and M3, which can be explained by the arrangement of the elements in the structure and the distribution of mass and inertial forces induced by the seismic action. However, it is noticeable that both M2 and M3 have almost the same response in the Y direction.
- As expected, the building which is regular in plan (M1) will in general have better response than the other two models (M2 and M3), which can be seen through the geometric mean fragility and vulnerability results.

## Acknowledgements

This work was supported by the Ministry of Education, Science and Technological Development of the Republic of Serbia (Contract No. 451-03-68/2022-14/200213 from 4.2.2022), (B. Folić).

## References

- [1] S. E. Naveen, N. M. Abraham, A. S. Kumari, Analysis of Irregular Structures under Earthquake Loads, 2nd International Conference on Structural Integrity and Exhibition 2018, Procedia Structural Integrity 14, 2019, pp. 806–819.
- [2] EN1998—Part 1, Eurocode 8: Design of Structures for Earthquake Resistance—Part 1: General Rules, Seismic Actions and Rules for Buildings; European Committee for Standardization (CEN): Brussels, Belgium, 2004.
- [3] P. Dewangan, T. Saxena, Seismic Analysis of Regular & Irregular Structures and its Comparison, Int. Research Journal of Engineering and Technology (IRJET) Volume: 05 Issue: 09, Sep 2018.
- [4] P. A. Krishnan, N. Thasleen, Seismic analysis of plan irregular RC building frames, IOP Conf. Ser.: Earth Environ. 2020, Sci. 491, 012021.
- [5] G. E. Manoukas Evaluation of a multimode pushover procedure for asymmetric in plan and non-regular in elevation R/C buildings, Elsevier, Soil Dynamics and Earthquake Engineering 115, 2018, pp. 742-775.
- [6] R. Folić, M. Čokić, Fragility and Vulnerability Analysis of an RC Building with the Application of Nonlinear Analysis. Buildings 2021, 11, 390. <https://doi.org/10.3390/buildings11090390>
- [7] EN 1990. ICS 91.010.30, Basis of Structural Design; European Committee for Standardization (CEN): Brussels, Belgium, 2005.
- [8] EN1991, Eurocode 1: Actions on Structures—Part 1-1: General Actions—Densities, Self-weight, Imposed Loads for Buildings; European Committee for Standardization (CEN): Brussels, 2002.
- [9] EN1992—Part 1, Eurocode 2: Design of Concrete Structures—Part 1-1: General Rules and Rules for Buildings; CEN: Brussels, Belgium, 2004.

- [10] EN1998—Part 2, Eurocode 8: Design of Structures for Earthquake Resistance—Part 2: Bridges; European Committee for Standardization (CEN), Brussels, Belgium, 2005.
- [11] EN1998—Part 3, Eurocode 8: Design of Structures for Earthquake Resistance—Part 3: Assessment and Retrofitting of Buildings; European Committee for Standardization (CEN): Brussels, 2004.
- [12] Z.V. Milutinović, G.S. Trendafiloski, RISK-UE, An advanced approach to earthquake risk scenarios with applications to different European towns. In Contract: EVK4-CT-2000-00014, WP4 Vulnerability of Current Buildings; 2003; 110p. Available online: [http://www.civil.ist.utl.pt/~mlopes/conteudos/DamageStates/Risk%20UE%20WP04\\_Vulnerability.pdf](http://www.civil.ist.utl.pt/~mlopes/conteudos/DamageStates/Risk%20UE%20WP04_Vulnerability.pdf) (accessed on 1st January 2021)
- [13] ETABS, version 17, Computers and Structures, Inc., Berkeley, California, USA, 2018.
- [14] J. Mander, M. Priestley, R. Park, Theoretical Stress-Strain Model for Confined Concrete. *J. Struct. Eng.* 1988, 114, 1804–1825.
- [15] K. A. Porter, *Beginner's Guide to Fragility, Vulnerability, and Risk*; University of Colorado Boulder: Boulder, CO, USA, 2015; doi:10.1007/978-3-642-35344-4\_256.
- [16] J.W. Baker, Efficient analytical fragility function fitting using dynamic structural analysis. *Earthq. Spectra* 2015, 31, 579–599.
- [17] D. D'Ayala, A. Meslem, D. Vamvatsikos, K. Porter, T. Rossetto, V. Silva, *Guidelines for Analytical Vulnerability Assessment of Low/Mid-Rise Buildings*. GEM Technical Report 2015-08 V1.0.0. GEM Foundation: Pavia, Italy, 2014, doi:10.13117/GEM.VULN-MOD.TR2014.12.